Interface Effects on the Vibrational Properties of 3C–InN/3C–AlN Superlattices

E. F. Bezerra, V. N. Freire, J. Mendes Filho, and V. Lemos
Departamento de Física, Universidade Federal do Ceará, Caixa Postal 6030, Campus do Pici, 60455-760 Fortaleza, Ceará, Brazil

Received on 23 April, 2001

Calculation of the Raman spectra of zinc–blende InN/AlN superlattices were carried out assuming the existence of an interface region with thickness δ varying from zero to three monolayers. Frequency shifts up to $80\,\mathrm{cm}^{-1}$ were observed for some of the optical frequencies when $\delta = 3$. Many peaks appearing at the low frequency side, shift toward the center position of the spectrum. As a consequence, pairs of the Raman modes become quasi–degenerate giving rise to highly prominent structures in the spectrum, for $\delta = 2$ and 3. These effects are tracked to localization of atomic displacements mainly at the interface regions.

Group III–nitride semiconductors quantum well (QW) structures in the fabrication of optoelectronic devices are currently known, being of great interest light emitting diodes (LEDs) and laser diodes (LDs) operating in the blue–green or violet region [1, 2]. The optical and electrical processes in GaN, AlN and InN based QW and superlattice (SL) structures are remarkably influenced by the existence graded interfaces. The indium concentration gradient across the $GaN/In_{0.43}Ga_{0.57}N/Al_{0.1}Ga_{0.9}N$ interfaces was measured recently using high–resolution transmission electron microscopy (HRTEM) [3], pointing to a typical GaN/InGaN interface width of 1 nm, while more than twice this value is the thickness of the InGaN/AlGaN interface. In the case of $GaN/Al_xGa_{1-x}N$ SL's, Raman scattering measurements provide evidence of the graded alloy interface region to be of the order of 2 nm [4].

Lattice dynamics calculations are available for bulk GaN, AlN and InN crystalized in the wurtzite and zinc–blende structures [5, 6], from which the calculated bulk phonon frequencies can be used in the simulation of the Raman scattering of their superlattices. Previous theoretical results show that interfacing effects are responsible for considerable gain in intensity of Raman modes in zinc–blende GaN/AlGaN SL's [7]. Even though the acoustic branch of bulk AlN overlap with the optical branch of InN, their optical dispersion curves do not overlap [6, 8]. Therefore, it is interesting to analyze the interface dependence of optical phonons in graded InN/AlN SLs.

The purpose of this work is to present a study on the phonon dispersion, atomic displacements and the Raman spectra of $(InN)_{8-\delta}/(InN_{0.5}AlN_{0.5})_\delta/(AlN)_{8-\delta}/(InN_{0.5}AlN_{0.5})_\delta$ SL's, with δ = 1,2,3. Most of the optical phonons were found to be confined in the abrupt SL probably due to non–overlapping optical branches of bulk constituents. For this reason, there is strong localization of modes in the InN/AlN interfaced SL's resulting in remarkable gain of the Raman intensity of these modes.

The vibrational properties of the InN/AlN SL are described through a modified linear chain model. Each atom in the linear chain model represents a plane of atoms in the actual SL, and their associated phonons propagating along the [001] axis can be described through a one–dimensional set of equations of motion. The bulk selection rules forbid TO modes in a backscattering geometry of a (001) face in a crystal with either a zinc–blende or a diamond structure. Symmetry arguments show that only the LO modes should play a role in the Raman scattering of a perfect superlattice constructed with those components [9]. The equations of motion can be solved in the harmonic approximation, and their eigenvalues and eigenvectors are obtained by diagonalization of the dynamical matrix. The force constants were obtained considering interaction to nearest and next–nearest–neighbors, only.

Alloyed interfaces in the virtual–crystal approximation were taken to describe the interface. This is appropriate for the one–mode–type behavior of longitudinal vibrations in the alloy. This behavior was assumed in the case of the LO modes of AlInN alloys based on previous demonstrations of the one–mode–type behav-

ior in other nitride based alloys studied either experimentally [10, 11, 12, 13, 14] or theoretically [6, 15, 16]. The interface was simulated with both constituents in equal proportion and its width was varied in steps of one monolayer up to $\delta = 3$. The bond–polarizability model [9], which provides a good description of optical modes, was used to calculate the Raman spectra of the SLs.

The polarizability constants were assumed to have fixed values throughout the SL. The bulk InN and AlN mode frequencies (as used in the linear chain model) and the force constants are listed in Table I. The AlN zone–centre LO frequency was taken as 902 cm^{-1} from experimental data of Harima *et al.* [10]. The acoustic LA frequency was taken as the theoretical value of Karch *et al.* [17]. The InN LO(Γ) frequency is taken as the value measured by using Raman scattering [18], while the zone edge phonon frequencies for this crystal were obtained from calculations [19].

Table I. Bulk AlN and InN mode frequencies as used in the model to derive the force constants k, q_1, and q_2. The frequency values are in units of cm^{-1}.

	GaN	InN
LO (Γ)	902.0 [a]	588.0 [c]
LO (X)	723.0 [b]	567.0 [d]
LA (X)	594.0 [b]	231.0 [d]
k	222.8	128.2
q_1	30.0	26.9
q_2	2.7	2.8

[a] From ref. [10]; [b] From ref. [17]; [c] From ref. [18]; [d] From ref. [19]

Calculated Raman spectra for zinc–blende $(InN)_{8-\delta}/\ (InN_{0.5}AlN_{0.5})_\delta/(AlN)_{8-\delta}/\ (InN_{0.5}AlN_{0.5})_\delta$ SL's are presented in Fig. 1 for several values of interface width δ. The lowest curve, for $\delta = 0$, shows two dominant peaks at $\omega = 568$ cm^{-1} (probably due to almost degenerated modes 17–19) and $\omega = 899$ cm^{-1} (mode 32). Last frequency is quasi–coincident with the LO bulk values of AlN. In between, several weak structures appear at $\omega = 669$ cm^{-1} and $\omega = 721$ cm^{-1}, $\omega = 754$ cm^{-1}, $\omega = 823$ cm^{-1} and $\omega = 873$ cm^{-1} corresponding to modes 24, 25, 26, 28 and 30, respectively. This identification was made by comparison of the Raman frequencies with the values found in the calculated dispersion relations.

The introduction of an interface with δ=1, results in a modified spectrum with an additional peak showing at $\omega = 610$ cm^{-1}, and a down shift in frequency for the remaining features in the middle range of the spectrum [600,870] cm^{-1}. This is shown in Fig. 1 (δ=1), where the arrows indicate modes 24, 25, 26, 28 and 30. A larger interface, of two monolayers, causes further increase of the number of peaks in the middle frequency range, with the appearance of mode 22 at $\omega = 607$ cm^{-1}. The same set of peaks as before, is indicated by arrows in the spectrum labeled δ=2 in Fig. 1. It can be noticed that the lower frequency peaks shifted upward (related to δ=1) while those of higher frequency shift downward, resulting in a more crowded middle range than in the case of δ=1. Figure 1 also shows a remarkable increase of the Raman intensity, particularly in the spectra for δ=2 at $\omega \simeq 685$ cm^{-1} and δ=3 at $\omega \simeq 698$ cm^{-1}. Notice that the new peak for δ=3 is of the same magnitude as those at the extremities of the spectrum.

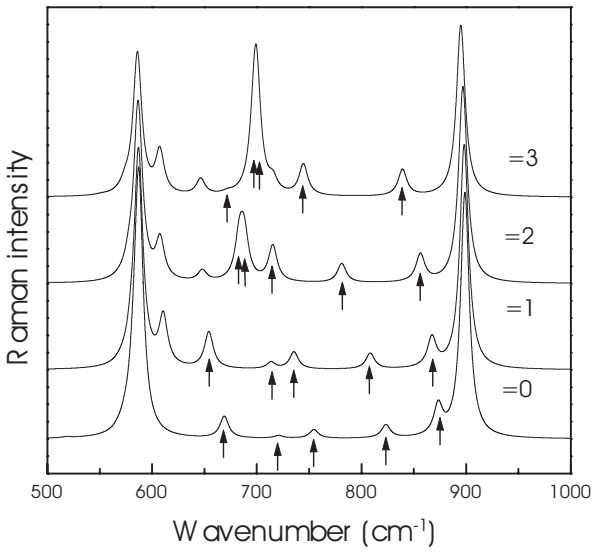

Figure 1. Calculated Raman spectra for zinc–blende $(InN)_{8-\delta}/(InN_{0.5}AlN_{0.5})_\delta/(AlN)_{8-\delta}/\ (InN_{0.5}AlN_{0.5})_\delta$ SL's.

An examination of the dependence of the number of modes with the frequency ω indicates that the unchanged frequencies correspond to vibrations basically unaffected by interfacing. Those with important frequency shifts should correspond to the most interface–affected modes, as far as localization of the vibration is concerned. To test this idea, we have calculated the atomic displacements in the superlattice, which are not presented here. We found most of the modes to be confined either in the InN layer or in the AlN layer for $\delta = 0$. Modes 17 and 18 are exceptions being extended for $\delta = 0$. It was also observed that the mode 24 is well localized at the InN/AlN interface for $\delta = 0$. Modes 19

to 23 are confined to the InN layer and the remaining modes to the AlN layer. Confinement of modes 25 to 32 are observed for $\delta = 1$. Interfacing was observed to produce localization of the modes, in general. For $\delta = 1$, the mode 23 is found to localize at the direct InN/AlN interface; for $\delta = 2$ it localizes at the inverse AlN/InN interface; and for $\delta = 3$ it localizes back at the direct interface. The mode 24 behaves in an inverted way, localizing at the opposed interfaces. Both modes lose, to a certain degree, the localized character for $\delta = 3$. This behavior is consistent with their Raman intensity being strong, particularly for $\delta = 1$ and $\delta = 2$. Mode 25 is well localized at the inverse interface at $\delta = 2$ and at the direct for $\delta = 3$. Mode 26 shows atomic displacements close to both interfaces for $\delta = 3$. Their corresponding increase in intensity can be checked in Fig. 1. It is worth mentioning that a previous calculation of the projected density of states for acoustic vibrations using the linear chain model shows a remarkable increase for the strongest localized modes leading to enhanced intensities [20].

Summarizing, interface effects on the Raman spectra of zinc–blende $(InN)_{8-\delta}/(InN_{0.5}AlN_{0.5})_{\delta}/(AlN)_{8-\delta}/(InN_{0.5}AlN_{0.5})_{\delta}$ SL's were studied using a linear chain description and the bond–polarizability model. It was shown that the optical modes region of the spectrum is severely affected by the existence of the interface regions. The main effect is the increase of intensity of peaks positioned in between those related to the end spectra modes. These peaks were seen to shift with increasing δ towards the center position in the spectrum. The $\delta = 3$ interface effects in the Raman intensities are drastic, giving rise to a most prominent structure in the middle frequency range of the spectrum. This structure results from the overlap of two quasi–degenerate modes. Examination of atomic displacements allowed for the effects to be tracked to localization of the vibrations. These effects are much stronger than those observed previously for other systems like GaAs/AlAs, Si/Ge, and AlN/GaN SL's. The optical modes are, therefore, well suited as probe for interfacing with both, frequency and intensity, highly affected.

Acknowledgments – The authors would like to acknowledge the Conselho Nacional de Desenvolvimento Científico e Tecnológico (CNPq), and Fundação de Amparo à Pesquisa do Estado do Ceará (FUNCAP), for financial support.

References

[1] S. Nakamura, Semicond. Sci. Technol. **14**, R27 (1999); *ibid The blue laser diode–GAN based light emitters and lasers* (Springer, Berlin 1997).

[2] F.A. Ponce and D.P. Bour, Nature (London) **386**, 351 (1997).

[3] C. Kisielowski, Z. Liliental–Weber, and S. Nakamura, Jpn. J. Appl. Phys. **36**, 6932 (1997).

[4] D. Behr, R. Niebuhr, J. Wagner, K.-H. Bachem, and U. Kaufmann, Appl. Phys. Lett. **70**, 363 (1997).

[5] G. Kaczmarczyk, A. Kaschner, S. Reich, A. Hoffmann, C. Thomsen, D.J. As, A.P. Lima, D. Schikora, K. Lischka, R. Averbeck, and H. Riechert, Appl. Phys. Lett. **76**, 2122 (2000).

[6] F. Bechstedt and H. Grille, Phys. Stat. Sol. **(b) 216**, 761 (1999).

[7] E. F. Bezerra, V. N. Freire, A. M. R. Teixeira, M. A. Araújo Silva, P. T. C. Freire, J. Mendes Filho and V. Lemos, Phys. Rev. B **61**, 13060 (2000).

[8] C. Bungaro, K. Rapcewicz, and J. Bernholc Phys. Rev. B **61**, 6720 (2000).

[9] B. Jusserand and M. Cardona, in *Light Scattering in Solids V*, edited by M. Cardona and G. Güntherodt, *Topics in Applied Physics*, Vol. **66**, p. 49 (Springer, Heidelberg, 1989).

[10] H. Harima, T. Inoue, S. Nakahima, O. Okumura, T. Ishida, S. Yoshida, T. Koizumi, H. Grille, and F. Bechstedt, Appl. Phys. Lett. **74**, 191 (1999).

[11] A. Tabata, J.R. Leite, A.P. Lima, E. Silveira, V. Lemos, T. Frey, B. Schöttker, D. Schikora, and K. Lischka, Appl. Phys. Lett. **75**, 1095 (1999).

[12] E. Silveira, A. Tabata, J. R. Leite, R. Trentin, V. Lemos, T. Frey, D. J. As, D. Schikora, and K. Lischka, Appl. Phys. Lett. **75**, 3602 (1999).

[13] T. Inushima, T. Shiraishi, and V.Y. Davydov, Solid State Commun. **110**, 491 (1999).

[14] M.S. Liu, Y.Z. Tong, Les A. Bursill S. Prawer, K.W. Nugent, and G.Y. Zhang, Solid State Commun. **108**, 765 (1998).

[15] H. Grille, and F. Bechstedt, J. Raman Spectrosc. **27**, 201 (1996).

[16] D.N. Tawar, Mater. Sci. Engineer. B **47**, 155 (1997).

[17] K.Karch, J.–M. Wagner, and F. Bechstedt, Phys. Rev. B **57** 7043 (1998).

[18] A. Tabata, A.P. Lima, L.K. Teles, L.M.R. Scolfaro, J.R. Leite, V. Lemos, B. Schöttker, T. Frey, D. Schikora, and K. Lischka, Appl. Phys. Lett. **74**, 362 (1999).

[19] F. Bechstedt, U. Grossner, and J. Furthmm̈uller, Phys. Rev. B **62**, 8003 (2000).

[20] V. Lemos, O. Pilla, and M. Montagna, J. Braz. Chem. Soc. **7**, 471 (1996).